

AxOMaP: Designing FPGA-based Approximate Arithmetic Operators using Mathematical Programming

SIVA SATYENDRA SAHOO, Interuniversity Microelectronics Centre (IMEC), Belgium

SALIM ULLAH and AKASH KUMAR, The Chair for Processor Design, Center for Advancing Electronics Dresden (CfAED), Technische Universität Dresden, Germany

With the increasing application of machine learning (ML) algorithms in embedded systems, there is a rising necessity to design low-cost computer arithmetic for these resource-constrained systems. As a result, emerging models of computation, such as approximate and stochastic computing, that leverage the inherent error-resilience of such algorithms are being actively explored for implementing ML inference on resource-constrained systems. Approximate computing (AxC) aims to provide disproportionate gains in the power, performance, and area (PPA) of an application by allowing some level of reduction in its behavioral accuracy (BEHAV). Using approximate operators (AxOs) for computer arithmetic forms one of the more prevalent methods of implementing AxC. AxOs provide the additional scope for finer granularity of optimization, compared to only precision scaling of computer arithmetic. To this end, the design of platform-specific and cost-efficient approximate operators forms an important research goal. Recently, multiple works have reported the use of AI/ML-based approaches for synthesizing novel FPGA-based AxOs. However, most of such works limit the use of AI/ML to designing ML-based surrogate functions that are used during iterative optimization processes. To this end, we propose a novel data analysis-driven mathematical programming-based approach to synthesizing approximate operators for FPGAs. Specifically, we formulate *mixed integer quadratically constrained programs* based on the results of correlation analysis of the characterization data and use the solutions to enable a more directed search approach for evolutionary optimization algorithms. Compared to traditional evolutionary algorithms-based optimization, we report up to 21% improvement in the hypervolume, for joint optimization of PPA and BEHAV, in the design of signed 8-bit multipliers. Further, we report up to 27% better hypervolume than other state-of-the-art approaches to DSE for FPGA-based application-specific AxOs.

CCS Concepts: • **Hardware** → **Circuit optimization**; *Hardware accelerators*; **Arithmetic and datapath circuits**; Software tools for EDA; • **Computing methodologies** → **Randomized search**.

Additional Key Words and Phrases: Approximate Computing, Arithmetic Operator Design, Circuit Synthesis, AI-based Exploration

1 Introduction

The last few years have witnessed a steady increase in both the extent and variety of applications using Machine Learning (ML). A large fraction of such applications involves deploying ML inference in embedded systems. To this end, the rising complexity of ML methods poses a complex problem for resource-constrained embedded systems. Consequently, computing paradigms such as Approximate Computing (AxC) and Stochastic Computing, which reduce the cost of computer arithmetic operations, are being actively explored. AxC denotes a wide variety of methods that can be implemented across the system stack and includes methods such as loop skipping, precision scaling, and load value approximation [8, 26, 28]. For the hardware layer, employing Approximate Operators (AxOs) for computer arithmetic forms an active area of research. AxOs provide an additional degree of freedom beyond the precision-scaling of arithmetic operations [8, 19, 22] and, similar to precision scaling, can provide large Power-Performance-Area (PPA) gains by leveraging the applications' inherent error-resilience to reduced behavioral accuracy (BEHAV). Since ML

Authors' addresses: Siva Satyendra Sahoo, Interuniversity Microelectronics Centre (IMEC), Leuven, Belgium, Siva.Satyendra.Sahoo@imec.be; Salim Ullah, salim.ullah@tu-dresden.de; Akash Kumar, The Chair for Processor Design, Center for Advancing Electronics Dresden (CfAED), Technische Universität Dresden, Dresden, Germany, akash.kumar@tu-dresden.de.

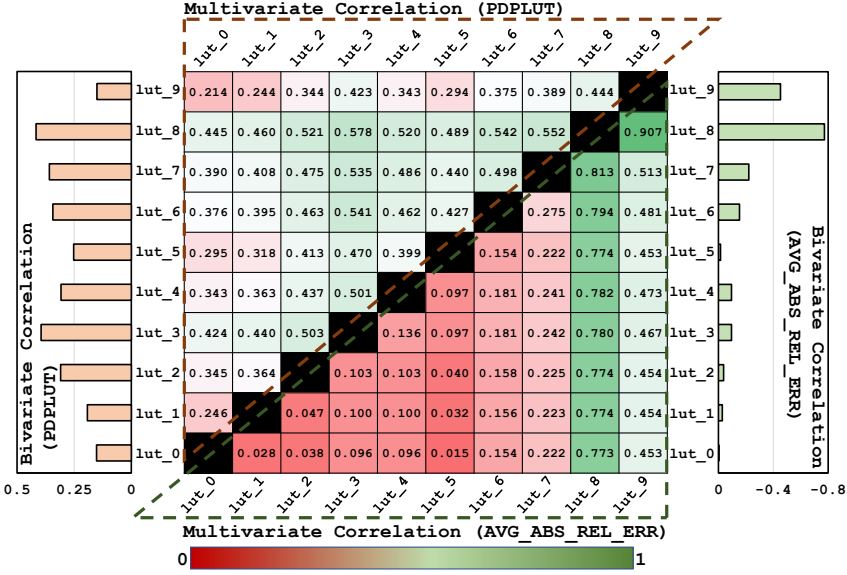


Fig. 1. Correlation between LUT usage and, PDPLUT and AVG_ABS_REL_ERR for approximate signed 4×4 multiplier designs obtained by selective LUT removal

inference primarily involves Multiply-Accumulate (MAC) operations, any PPA gains of arithmetic operator implementation can result in considerable system-level PPA improvements.

Designing AxOs for computer arithmetic usually entails avoiding the implementation of some part of the processing while still ensuring good enough behavioral accuracy. This approach is unlike precision scaling, where the operands are scaled to a different bit-width representation scheme. Further, precision scaling limits the scope of exploration to just a few possible bit widths. Using AxOs, on the other hand, provides a much finer granularity of implementation and, as a result, can provide larger scope for application-specific optimizations. However, the finer granularity of design and implementation also results in a much larger design space. For instance, as shown in [10], each combinatorial removal of logic gates in implementing an operator can result in a unique AxO. The consideration of the hardware platform for implementing AxOs further exacerbates the corresponding Design Space Exploration (DSE) problem. For instance, AxOs designed for Application-specific Integrated Circuits (ASICs) do not necessarily result in equivalent gains when implemented on Look-Up Table (LUT)-based Field Programmable Gate Arrays (FPGAs) and vice versa [16, 24, 27].

Given the diversity of applications being implemented in embedded systems, FPGAs provide the best PPA and time-to-market (cost) trade-offs. As a result, FPGAs are being increasingly used at every scale of computing, from TinyML to compute servers [12, 18]. In this regard, using AxOs for error-tolerant applications can provide further performance and energy benefits across every scale of computation. In our current article, we limit the discussion to the design of FPGA-based AxOs. The DSE for such AxOs has ranged from implementing ASIC-optimized designs on FPGAs to optimizing the implementation of AxOs that consider the LUT and Carry-chain (CC) logic primitives of FPGAs. Recently ML-based methods have been proposed for the corresponding DSE problem. However, most of the approaches do not leverage any form of data analysis of the characterization data. We present a case study for motivating the use of correlation analysis in generating quantitative metrics that can be used in the DSE of FPGA-based AxOs.

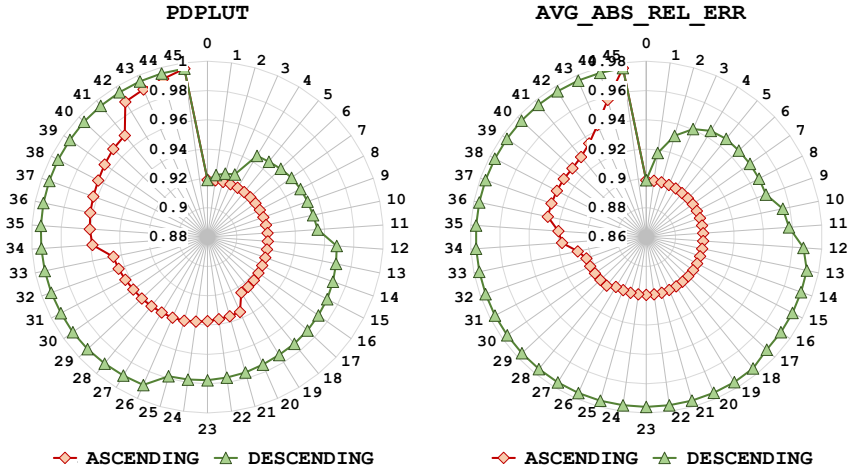


Fig. 2. Comparing the R^2 score of the polynomial regression models of PDPLUT and AVG_ABS_REL_ERR of approximate signed 4×4 multipliers with an increasing number of quadratic terms

Fig. 1 shows the results of the correlation analysis between LUT-usage and PDPLUT¹ and AVG_ABS_REL_ERR² metrics in the design of approximate signed 4×4 multipliers. The characterization data corresponds to the 1024 possible designs with the operator model presented in [25]. Accordingly, 10 LUTs in the implementation of the accurate design were marked for selective removal to generate approximate designs. The bar charts at either end of the figure show the *bivariate correlation* between each LUT’s usage³ and the corresponding PPA and BEHAV metrics. The heatmap in the figure shows the *multivariate correlation* when two LUTs were considered together in the design of an approximate version of the operator. Any cell in the upper left and bottom right triangle represents the joint correlation of the LUTs corresponding to the row and column index of the matrix with the PPA and BEHAV metric, respectively. As can be seen in the figure, there is a non-uniform correlation, and the analysis provides some indication of the contribution of each LUT to the PPA and BEHAV metrics. For example, LUT₈ and LUT₉ show a comparatively higher impact on the BEHAV. Similarly, for the PDPLUT metric various LUTs show a comparatively more substantial effect.

We used the multivariate correlation data to rank the joint LUTs (say lut_x and lut_y) and progressively added the product of the corresponding LUTs (lut_x × lut_y) as an additional feature in the Polynomial Regression (PR) model for predicting the PPA and BEHAV metrics. Fig. 2 shows the progression of the R^2 score (training) of the PR model for both metrics. The point 0 on the radial axis corresponds to a linear regression model, and the other points represent using one additional quadratic feature. The red and green points correspond to the results when the quadratic features were sorted in ascending and descending order, respectively. As evident, adding quadratic features with higher correlation results in a faster increase in the prediction capability of the model. This motivates the use of statistical analysis of characterization data for DSE. To this end, we present AxOMaP, a methodology to leverage correlation analysis in the design of FPGA-based AxOs. The related contributions are listed below.

¹PPA: Power × CPD × LUT usage

²BEHAV: Average absolute relative error

³Using 1/0 to represent the usage/removal of each LUT respectively

Contributions:

- (1) We present a novel approach to formulating the synthesis of FPGA-based approximate operators as a Mathematical Programming (MaP) problem. Specifically, we use the correlation analysis to formulate a Mixed Integer Quadratically Constrained Program (MIQCP) problem to generate approximate design configurations.
- (2) We present an augmented meta-heuristics optimization method for the corresponding DSE problem. Specifically, we use results from solving the MIQCPs to direct a Genetic Algorithms (GA)-based search on generating better design points than generic evolutionary optimization approaches.
- (3) We evaluate the proposed methodology for both operator-level and application-specific DSE. Compared to traditional evolutionary algorithms-based optimization, we report up to 21% improvement in the hypervolume, for joint optimization of PPA and BEHAV, in the design of signed 8-bit multipliers. Further, we report up to 27% better hypervolume than other state-of-the-art approaches to DSE for FPGA-based application-specific approximate operators.

The rest of the article is organized as follows. Section 2 presents a brief overview of the requisite background and related works. The operator model used in the analysis is presented in Section 3. Section 4 presents the various components and methods of the proposed *AxOMaP* methodology. The analysis of the results of the experimental evaluation of the proposed methods is presented in Section 5. Finally, in Section 6, we conclude the article with a summary and a brief discussion of the scope for related future research.

2 Background and Related Works

2.1 Approximate Computing

Approximate Computing (AxC) paradigm has proven to be a feasible solution to address the ever-increasing computational and memory needs of modern applications ranging from data centers to embedded systems at the edge. Most of these application domains, such as machine learning, computer vision, data mining, and synthesis, offer an inherent error tolerance to the inaccuracies (approximations) in their computations [28]. AxC uses this error tolerance to trade the output accuracy of an application for performance gains. Recent related works have presented various approximation techniques that cover all layers of the system stack [8, 22]. However, for the resource-constrained embedded systems, the architecture and circuit layers have remained the focus of recent related works. For example, employing reduced precision operations is the most commonly employed architectural-level technique [1, 29, 31]. Similarly, using approximate computational units is one of the most commonly used and useful techniques on the circuit layer. Furthermore, as MAC is one of the main operations in error-tolerant applications, such as ML, computer vision, and digital signal processing, most related works have proposed various approximate implementations for adders and multipliers [3, 10, 11, 17, 19, 21, 24, 25, 27, 30].

Most of AxO architectures primarily rely on intentionally introducing approximations for performance gains by truncating portions of some of the calculations or employing inaccurate computations. For example, the authors of [21, 30] have proposed to utilize multiple sub-adders to truncate long carry-propagation chains in larger adders. These designs employ multiple preceding bits for each sub-adder to improve the overall accuracy of the larger adder. Similarly, the work presented in [17] has proposed a set of FPGA-optimized approximate adders by using various carry and sum prediction methods.

The majority of related works have focused on the multiplication operation, owing to its high computational complexity, and proposed various ASIC- and FPGA-optimized architectures. For

TABLE 1. Comparing related works

Related Works	[10, 11]	[27]	[9]	[16]	[25]	[19]	AxOMaP
LUT-level Optimization	✗	✓	✗	✗	✓	✓	✓
Application-specific DSE	✗	✗	✓	✓	✓	✗	✓
Automated Search	✓	✗	✓	✗	✓	✓	✓
ML-based Estimation	✗	✗	✓	✓	✓	✓	✓
Iterative Search	✓	✓	✓	✓	✓	✗	✓
Directed Search	✗	✗	✗	✗	✗	✗	✓

instance, the works proposed in [6, 14] have used various truncation strategies to implement an $M \times M$ multiplier by producing an M -bit output. Similarly, other works, such as [5], rely on truncating the input operands to utilize comparatively smaller multipliers to implement a larger multiplier. Other techniques, such as those proposed in [20] and [7] have utilized functional approximation to implement ASIC-optimized inaccurate 2×2 multipliers. The optimized 2×2 modules are then utilized to implement larger multipliers. The authors of [10] and [11] have employed Cartesian Genetic Programming (CGP) to present ASIC-optimized approximative adders and multipliers libraries. In their proposed work, they generate approximate operators by executing multiple iterations of the CGP on a set of accurate implementations of an operator. For the CGP iterations, the accurate circuits are represented as strings of numbers, and various approximations of an operator are created using a worst-case error-based objective function. Considering the architectural details of FPGAs, the authors of [27], [24], and [23] have proposed various LUT-level optimization to implement approximate multiplier architecture optimized for Xilinx FPGAs. The techniques presented [24] and [23] have proposed 4×4 approximate multipliers as the building blocks to implement higher-order multipliers. Compared to the ASIC-optimized 2×2 designs, LUT-optimized 4×4 multipliers utilize LUTs more efficiently. The work presented in [27] has focused on implementing signed approximate multipliers. For this purpose, the proposed work uses a radix-4 booth algorithm and employs both functional approximation and truncation of product bits to reduce the total number of utilized LUTs and carry-propagation chains.

2.2 DSE for Approximate Operators

Some recent works, such as [9, 16, 19, 25], have employed various techniques to provide libraries of approximate arithmetic operators with varying accuracy-performance trade-offs. These libraries often offer thousands of approximate versions of a single arithmetic operator. For example, the work in [25] can provide up to 2^{36} approximate signed 8×8 multipliers. Therefore, in many cases, it is rather challenging to identify a feasible implementation of an operator that can satisfy the provided accuracy-performance constraints. For example, the work presented in [27] has utilized GA to find feasible operator implementations for a Gaussian image smoothing application. Similarly, the authors of [19] have used Generative Adversarial Networks (GANs) to find operator configurations meeting provided accuracy-performance constraints. Table 1 summarizes the different aspects explored by related works for the DSE of FPGA-based AxOs.

While earlier works had focused on implementing ASIC-optimized designs on FPGAs [9, 16], more recent works have focused on synthesizing novel AxOs that leverage the LUT and CC-based architecture of FPGAs [3, 19, 25, 27]. Across both approaches, recent works have shown increased

usage of AI/ML-based methods in the DSE [9, 16, 19, 25]. However, this has been primarily limited to using ML-based estimators of PPA and BEHAV metrics as surrogate fitness functions in iterative optimization methods. Only [19] implements a purely ML-based generation of novel AxO designs. However, due to the *open-loop*⁴ nature of this approach, it can suffer from degraded search results. Also, a considerable amount of computations(training) are needed for designing the generative networks. Further, none of the works discussed above use any knowledge/information derived from the characterization data to enhance the DSE search. Therefore, we posit that *the results from the data analysis of the characterization data along with low-cost mathematical programming can be used to improve the efficacy of iterative/randomized optimization algorithms*. To this end, AxOMaP provides a methodology for enabling such improvements in evolutionary algorithms-based optimization.

⁴The fitness of newly generated designs is not fed back to the model for iterative improvement

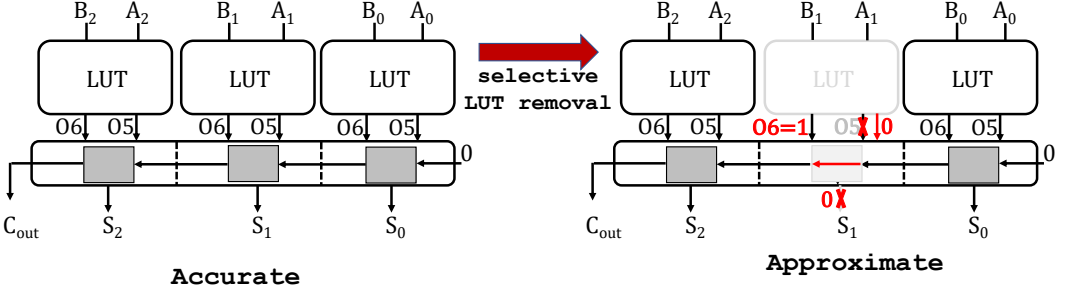


Fig. 3. Approximating a 3 – bit unsigned adder’s FPGA implementation using selective LUT removal

3 Operator Model

The operator model used in the current article is similar to that proposed in [25]. Accordingly to the model, any FPGA-based arithmetic operator can be represented by an ordered tuple:

$$O_i(l_0, l_1, \dots, l_l, \dots, l_{L-1}), \forall l_i \in \{0, 1\}$$

The term l_i represents whether the LUT corresponding to the operator’s accurate implementation is being used or not and L represents the total number of LUTs of the accurate implementation that may be removed to implement approximation. Therefore, $O_{Ac}(1, 1, \dots, 1)$ represents the accurate implementation. For instance, the accurate implementation of the 3-bit unsigned adder, shown in Fig. 3, is represented by the tuple $(1,1,1)$, and $\mathcal{O} = \{O_i\}$ represents the set of all possible implementations of the operator. Accordingly, the set \mathcal{O} for the adder shown in the figure is $\{(0,0,0), (0,0,1), (0,1,0), (0,1,1), (1,0,0), (1,0,1), (1,1,0), (1,1,1)\}$. The approximate implementation in the figure corresponds to the tuple $(1,0,1)$ where the middle LUT and the associated inputs are not used. Similarly, the output of the associate carry chain cell is also truncated. We can abstract any arbitrary operator/application’s behavior by a function \mathcal{S} . So, the operator/application output for a set of inputs can be outlined as shown in Eq. (1). The term Err_{O_i} represents the reduction in the operator/application’s behavioral accuracy, BEHAV, as a result of using an approximate operator O_i , compared to using the accurate operator O_{Ac} . Similarly, the operator/accelerator’s PPA can be abstracted as a set of functions as shown in Eq. (2).

$$\begin{aligned} Out_{O_i} &= \mathcal{S}(O_i, Inputs); Out_{O_{Ac}} = \mathcal{S}(O_{Ac}, Inputs) \\ Err_{O_i} &= Out_{O_{Ac}} - Out_{O_i} \end{aligned} \quad (1)$$

$$\begin{aligned} \text{Power Dissipation : } \mathcal{W}_{O_i} &= \mathcal{H}_W(O_i, Inputs) \\ \text{LUT Utilization : } \mathcal{U}_{O_i} &= \mathcal{H}_U(O_i) \\ \text{Critical Path Delay : } C_{O_i} &= \mathcal{H}_C(O_i) \\ \text{Power Delay Product : } PDP_{O_i} &= \mathcal{W}_{O_i} \times C_{O_i} \\ PDPLUT_{O_i} &= \mathcal{W}_{O_i} \times \mathcal{U}_{O_i} \times C_{O_i} \end{aligned} \quad (2)$$

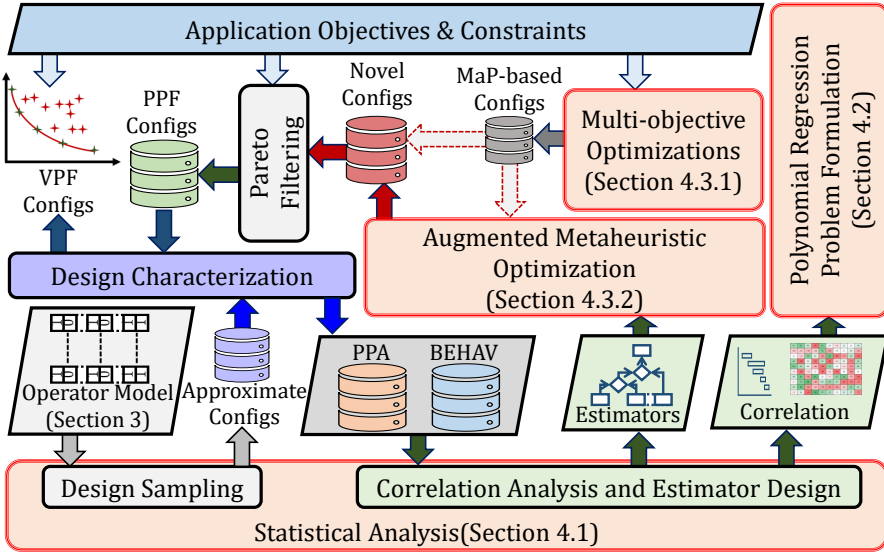


Fig. 4. AxOMaP Methodology

4 AxOMaP

The various processes and flow of information in the proposed AxOMaP methodology are shown in Fig. 4. The proposed contributions are highlighted with the relevant section numbers in the article. The statistical analysis involves generating the characterization data used in the correlation analysis and design of the ML-based estimators. The results of correlation analysis are used in the PR design and problem formulation. A set of problems are solved for each constrained multi-objective DSE problem to generate MaP-based approximate configurations. These configurations are then passed on as initial solutions for MaP-augmented metaheuristic optimization. The resulting solutions are Pareto-filtered using the estimators to generate the Pseudo Pareto-front (PPF) design configurations which are then characterized (synthesis and implementation) to generate the Validated Pareto-front (VPF) of FPGA-based AxOs.

4.1 Statistical Analysis

4.1.1 Dataset Generation We used the operator model presented in AppAxO [25] to generate a number of approximate designs for characterization and further data analysis. While random sampling (with uniform distribution) has been used in related works, we observed a skewed distribution of the resulting metrics. For instance, Fig. 5 shows the distribution of the PDPLUT and AVG_ABS_REL_ERR of the set of all possible signed 4×4 multiplier designs that can be generated using the operator model. With random sampling in larger operators, the generated points followed a similar distribution, with most points lying within a narrow range for the PPA metrics. Consequently, in order to get a wider range of distribution, we augmented the randomly sampled dataset with design points generated by using different patterns, such as moving windows of consecutive and/or alternating ones and zeros.

4.1.2 Correlation Analysis The results of the correlation analysis for approximate designs of signed 4×4 multipliers were presented in Fig. 1. While the bivariate correlation data was generated by measuring the Pearson correlation coefficient, the multivariate correlation was generated using 1. The multivariate correlation essentially represents the capability of the selected independent

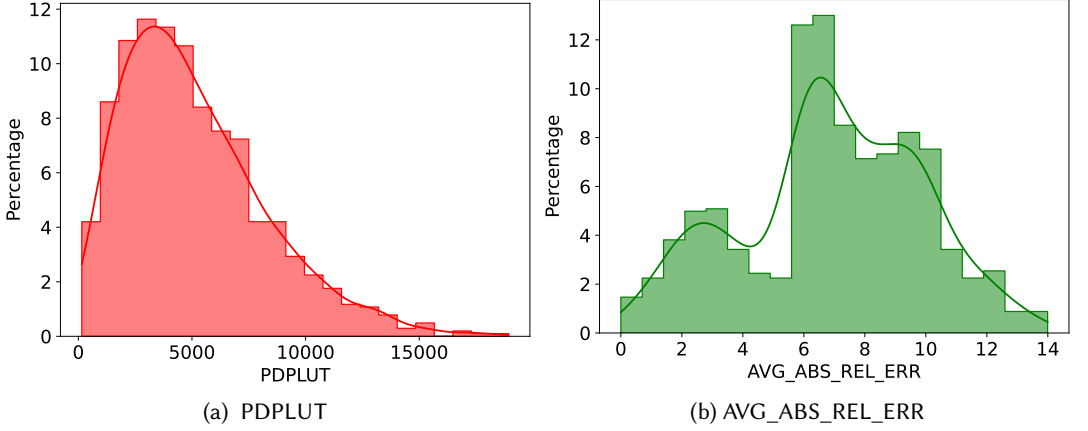


Fig. 5. Distribution of the PDPLUT and AVG_ABS_REL_ERR for 1024 approximate signed 4×4 multipliers generated using the operator model proposed in [25]

Algorithm 1 Computing multivariate correlation coefficient

Require: \mathcal{D} , x , y , \mathcal{M}

Metric under consideration: \mathcal{M}

Characterization dataset: $\mathcal{D}: \{(O_i, M_i)\}$

Arbitrary approximate configuration: O_i

Selected LUTs: x , y

- 1: Filter columns based on selected LUTs: x , y
 - 2: Train Regression model: $\mathcal{M} = c_0 + c_1 \times l_x + c_2 \times l_y$
 - 3: Compute R^2 score of the regression model: r^2
 - 4: Return $r = \sqrt{r^2}$
-

variables (features/LUTs) to predict the dependent variable (PPA/BEHAV metric) in a linear regression model. Therefore, as shown in 1, the square root of the R^2 score of the corresponding linear regression model, with the selected variables, is used to represent the multivariate correlation coefficient.

4.1.3 Estimator Design The current article focuses on using the characterization data more efficiently than just being limited to designing surrogate functions for estimating PPA and BEHAV metrics. Therefore, we used AutoML [15] to explore across ML models and their respective hyperparameters to determine the best estimator for each metric.

4.2 Problem formulation

The MaP aspect of AxOMaP involves using Polynomial Regression (PR) to generate Mixed Integer Linear Programming (MILP) and Mixed Integer Quadratically Constrained Program (MIQCP) problems.

4.2.1 Variables According to the operator model discussed in Section 3, the LUT usage determines the approximate design completely. Therefore, the LUT usage variables, $l_i, \forall i \in \{0, 1, 2, \dots, L-1\}$ forms the set of decision variables of the problem. Further, since we consider multi-objective optimization problems, i.e. minimizing one PPA metric and one BEHAV metric, we use two support

variables to represent the metrics, v_{ppa} and v_{behav} . The expression for these support variables is based on the polynomial regression results. Let us denote the set of PR coefficients as $p_{i,j}$ and $b_{i,j}$ where $p_{i,j}$ and $b_{i,j}$ represent the coefficients of the terms of the PR model of PPA and BEHAV respectively. For a linear model (and the corresponding MILP problem) we constraint $i = j$. Since we consider only binary decision variables, $l_i \times l_j$ is equivalent to l_i for $i = j$. The corresponding expression for v_{ppa} and v_{behav} are shown in Eq. (3). If we allow quadratic terms in the PR models, for MIQCP problems, we use the relationship shown in Eq. (4).

$$\begin{aligned} v_{ppa} &= \sum_{i=0}^{L-1} p_{i,i} \times l_i \\ v_{behav} &= \sum_{i=0}^{L-1} b_{i,i} \times l_i \end{aligned} \quad (3)$$

$$\begin{aligned} v_{ppa} &= \sum_{(i,j) \forall i,j \in \{0,1,\dots,L-1\}} p_{i,j} \times l_i l_j \\ v_{behav} &= \sum_{(i,j) \forall i,j \in \{0,1,\dots,L-1\}} b_{i,j} \times l_i l_j \end{aligned} \quad (4)$$

4.2.2 Constraints The set of constraints is shown in Eq. (5). The first set of constraints corresponds to the binary nature of the decision variables. The second set of constraints corresponds to the constraints set on the PPA and BEHAV metrics.

$$\begin{aligned} l_i &\in \{0, 1\} \forall i \in \{0, 1, \dots, L - 1\} \\ v_{behav} &\leq \max_{behav} ; v_{ppa} \leq \max_{ppa} \end{aligned} \quad (5)$$

4.2.3 Objective Eq. (6) shows the generic representation of the multi-objective optimization problem. Specific formulations to generate a solution pool are discussed next.

$$\begin{aligned} &\text{minimize}_{O_i \in O} (BEHAV_{O_i}, PPA_{O_i}) \\ &\text{s.t. } BEHAV_{O_i} \leq B_{MAX} \text{ and } PPA_{O_i} \leq P_{MAX} \end{aligned} \quad (6)$$

4.3 Generating Pareto-front Designs

4.3.1 Generating Solution Pool In order to generate a pool of solutions for each optimization problem, we use a weighted sum of the BEHAV and PPA metrics to formulate multiple objective functions. Eq. (7) shows the objective function used for each MaP problem. We sweep the value of wt_B from 0 to 1 in increments of 0.05, to generate nearly 20 optimization problems. Further, we also vary the number of quadratic features in the support variable expressions of Eq. (4) to generate multiple MaP problems. We used the multivariate correlation coefficients to rank the product features and incrementally add one additional feature to Eq. (3) to generate a new MaP problem. The corner cases of this approach are the MILP where no quadratic features are used and the case where all possible quadratic terms are included in Eq. (4). For approximating the signed 4×4 multiplier, with 10 removable LUTs, it results in 45 quadratic terms. Similarly, for a signed 8×8 multiplier with 36 removable LUTs it amounts to 630 quadratic terms. Hence, for larger designs

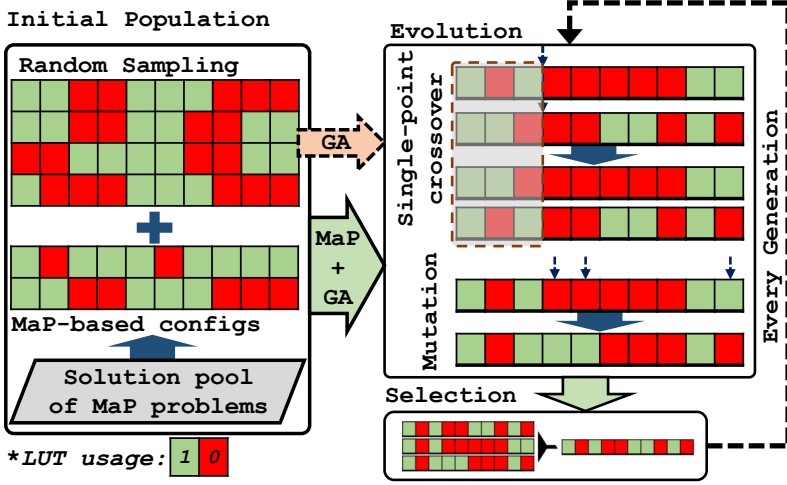


Fig. 6. Genetic Algorithms-based multi-objective DSE approaches explored in AxOMaP for synthesizing approximate operators

using all possible quadratic terms can result in large MaP problems, and the correlation analysis can be used to select a subset of the possible terms for the problem formulation.

We used the maximum PPA and BEHAV metrics reported in the training dataset, denoted by P_{MAX} and B_{MAX} respectively, to formulate different constrained optimization problems. Specifically, we use constraint scaling factor, $const_sf$, values of 0.2, 0.5, 0.8, 1.0, 1.2, and 1.5 to determine the max_{ppa} and max_{behav} of Eq. (5), as shown in Eq. (8). Each value of $const_sf$, and the resulting constrained optimization problem solutions indicate the efficacy of the DSE approach of the solver under different degrees of tight constraints.

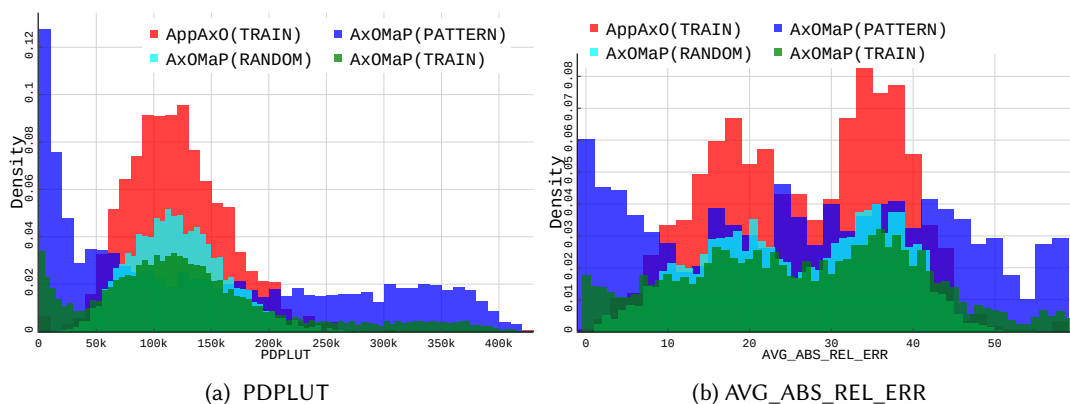
$$\underset{O_i \in \mathcal{O}}{\text{minimize}}(wt_B \times BEHAV_{O_i} + (1 - wt_B)PPA_{O_i}) \quad (7)$$

$$\begin{aligned} max_{ppa} &= const_sf \times P_{MAX} \\ max_{behav} &= const_sf \times B_{MAX} \end{aligned} \quad (8)$$

4.3.2 Augmented Metaheuristic Optimization We use GA as an example of a metaheuristics-based solver for the DSE of FPGA-based AxOs. GA involves generating an initial population of sample solutions and selecting the population for the next generation from a set of solutions obtained by crossover and mutation of the current population. We used tournament selection and single-point crossover with a maximum of 250 generations for each experiment. As shown in Fig. 6, the problem-agnostic GA method involves using random sampling to generate the initial population. We also use an augmented approach where we use the solutions pool generated by solving the MaP problems as the initial population, in addition to the random initial configurations. This allows us to direct the search towards pseudo-optimal solutions faster using MaP.

TABLE 2. Designs used for experiments

Design	Description	Accelerator	PPA metric	BEHAV Metric
OP	Signed 8×8 Multiplier	OP	PDPLUT	AVG_ABS_REL_ERR
ECG	Low-pass filter in ECG peak detection	1D Conv	PDPLUT	Peak detection error
MNIST	Last dense layer in MNIST digit recognition	GEMV	PDPLUT	Classification error
GAUSS	Gaussian smoothing using 2D convolution	2D Conv	PDPLUT	Average reduction in PSNR

Fig. 7. Comparison of the distribution of PDPLUT and AVG_ABS_REL_ERR for approximate signed 8×8 multipliers obtained by different methods of generating the characterization dataset

5 Experiments and Results

5.1 Experiment Setup

Table 2 shows the designs used for the experimental evaluation along with the relevant PPA and BEHAV metric used in each case. We use the implementation of approximate signed 8×8 multipliers, both as application-agnostic (OP) and as application-specific, designs for the experiments. These approximation configurations are implemented in VHDL and synthesized for the 7VX330T device of the Virtex-7 family using Xilinx Vivado 19.2. The dynamic power is computed by recording the dynamic switching activity for all possible input combinations of the multiplier configurations. For this purpose, we have used Vivado Simulator and Power Analyzer tools. The MaP and DSE methods are implemented in Python, utilizing packages such as DEAP [4], PyGMO [2] and Scikit [13] among others.

5.2 Statistical Analysis

5.2.1 Characterization Dataset Fig. 7 shows the distribution of PDPLUT and AVG_ABS_REL_ERR of approximate signed 8×8 multiplier designs generated using different approaches. The AppAxO (TRAIN) [25] and the AxOMaP (RANDOM) datasets show similar distributions as they follow primarily a uniform distribution-based random sampling. The AxOMaP (PATTERN) refers to the dataset generated as described in Section 4.1. Evidently, it results in a more balanced

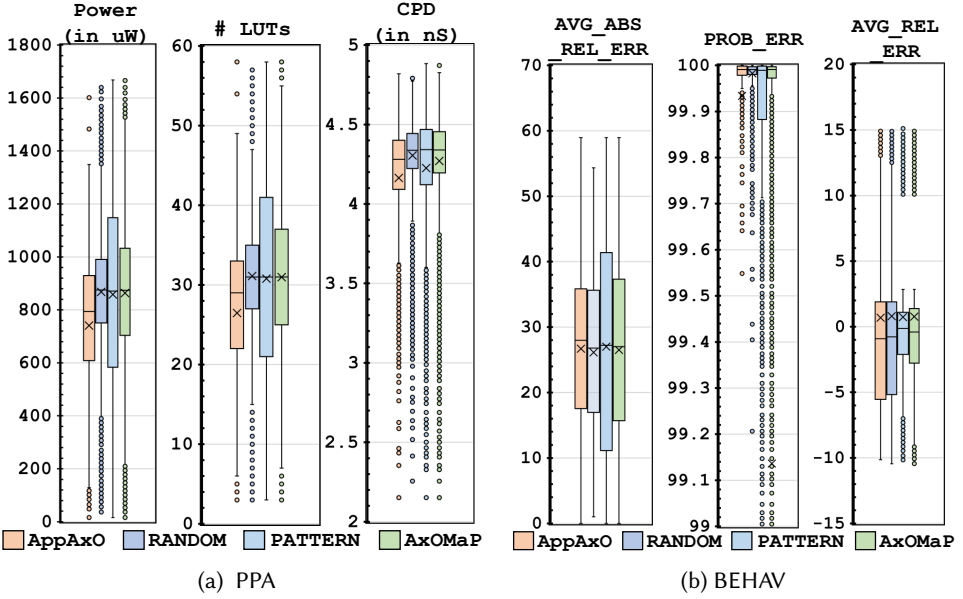


Fig. 8. Comparison of the distribution of multiple PPA and BEHAV metrics for approximate signed 8×8 multiplier for *AppAxO* [25] and *AxOMaP* training datasets

distribution across a wider range of the PPA metrics. The *AxOMaP*(TRAIN) refers to the dataset used for further analysis and modeling and combines the RANDOM and PATTERN datasets. Fig. 8 shows the box plots of various PPA and BEHAV metrics for the *AppAxO* and *AxOMaP* datasets. The *AxOMaP* dataset exhibits a wider range across all metrics. Specifically, for the *Probability of Error* (PROB_ERR) we observe many design points under 99.4%, while the *AppAxO* dataset has none. While some of the improvements result from the larger dataset (10,650 compared to 2000), most of the improvements result from the PATTERN dataset, which shows a wider range across most metrics.

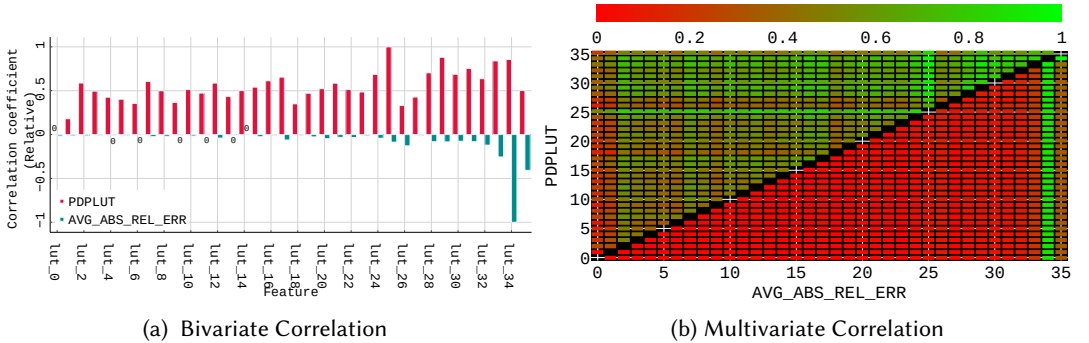


Fig. 9. Results of bivariate and multivariate correlation analysis of the training dataset of signed 8×8 approximate multipliers

5.2.2 *Correlation Analysis* Fig. 9 shows the results of the correlation analysis of the characterized dataset for approximate signed 8×8 multipliers. Fig. 9(a) shows the relative bivariate correlation

coefficients, of each of the 36 removable LUTs, with PDPLUT and AVG_ABS_REL_ERR. Similar to the data shown for the signed 4×4 multipliers presented in Fig. 1, the correlation coefficients for PDPLUT show a wider distribution across LUTs’ usage than AVG_ABS_REL_ERR, where a few LUTs show much larger correlation coefficient values than others. This imbalance is also reflected in the multivariate correlation data shown in Fig. 9(b) where the LUTs with higher bivariate correlation coefficients show higher multivariate correlation when analyzed alongside other LUTs.

5.2.3 Estimator Design Table 3 shows the results of AutoML for different PPA and BEHAV metrics for the approximate signed 8×8 multiplier characterization dataset. Since the features (LUT usage) are primarily categorical than numerical, ML algorithms that are tailored for categorical features, such as CatBoost, show better performance in the regression models. Almost all models (except for CPD) show R^2 scores of more than 0.9 across training and testing datasets. Also, metrics that are products of other metrics, such as PDP and PDPLUT, exhibit much higher Mean Squared Error (MSE) and Mean Average Error (MAE) values than others.

TABLE 3. Regression model metrics for various PPA and BEHAV metrics of approximate implementations of signed 8×8 multipliers

Model Metric		MSE		MAE		R2 Score	
Design Metric	Selected Model	TRAIN	TEST	TRAIN	TEST	TRAIN	TEST
AVG_ABS_ERR	CatBoost	396	5582	14	54	0.999	0.999
AVG_ABS_REL_ERR	CatBoost	0.015	0.03	0.088	0.125	0.999	0.999
PROB_ERR	LightGBM	0.289	1.505	0.122	0.293	0.989	0.929
POWER	CatBoost	206	768	11	22	0.998	0.992
CPD	LightGBM	0.012	0.018	0.086	0.104	0.877	0.819
LUTs	CatBoost	0.04	0.108	0.158	0.257	0.999	0.999
PDP	CatBoost	1596	6797	30	64	0.999	0.997
PDPLUT	CatBoost	6.6E6	1.4E6	1951	2909	0.999	0.998

5.3 Design Space Exploration

5.3.1 MaP-based DSE The design space exploration approach proposed in the current article comprises of generating a set of solutions to the constrained multi-objective optimization problem using MaP and then using the solutions from the MaP-based DSE to augment an evolutionary search. Fig. 10 shows the R^2 score and MAE values (for TRAIN and TEST) for the PR models used in formulating the MaP problems for DSE of approximate signed 8×8 multipliers. The PPA and BEHAV correspond to PDPLUT and AVG_ABS_REL_ERR respectively and each data point corresponds to adding one additional quadratic term. Hence, the graph plots results for problems with zero (MILP) to 630 quadratic terms, similar to the results for the signed 4×4 multipliers (shown in Fig. 2), the R^2 score for the training data increases with the addition of each quadratic terms.

However, the TEST R^2 score starts to decline after ~ 200 terms. This can be attributed to the lack of the generalization of PR models in predicting AVG_ABS_REL_ERR and resulting in overfitting. Fig. 11 shows the total hypervolume (TOT_HV) of the PPF and the minimum and maximum PDPLUT (MIN_/MAX_PPA) and AVG_ABS_REL_ERR(MIN_/MAX_BEHAV) reported in the solutions of the MaP problems corresponding to constraint scaling factor, *const_sf*, of 0.5. As observed, the highest hypervolume is reported with the addition of the first few quadratic terms. Adding more terms results in increasing the complexity of the MaP problems and may result in degraded results. However, using multiple problems allows us to generate a solution pool that can be used for further exploration.

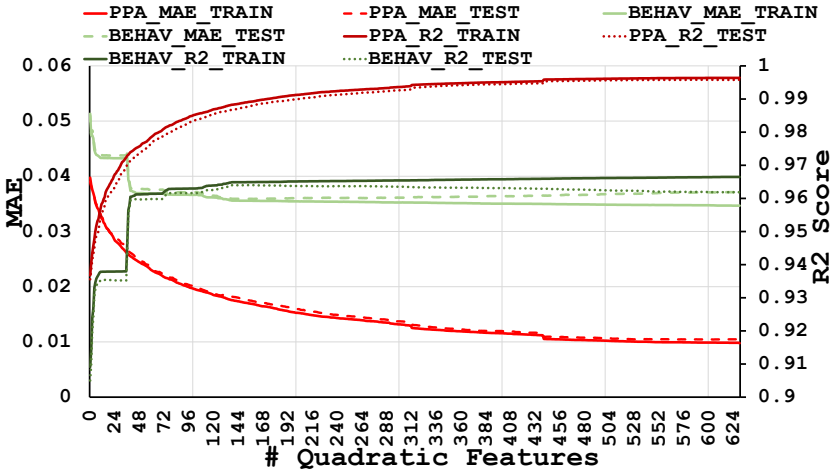


Fig. 10. Accuracy metrics of polynomial regression models with an increasing number of quadratic terms. *MinMaxScaling* was used before generating the models. PPA and BEHAV refer to PDPLUT and AVG_ABS_REL_ERR respectively

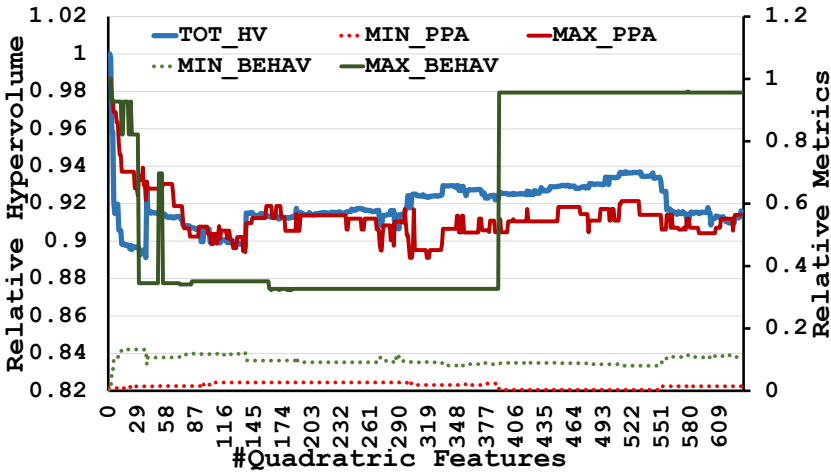


Fig. 11. PPF hypervolume (TOT_HV) and the maximum and minimum PDPLUT(PPA) and AVG_ABS_REL_ERR (BEHAV) reported in the solutions generated by the MaP problems using the polynomial regression models with an increasing number of quadratic terms

5.3.2 MaP-augmented DSE In addition to generating designs using MaP, we also used a MaP-augmented metaheuristic optimization. Fig. 13 shows the progression of the hypervolume in two methods of GA-based searches: (a) *GA only*: problem agnostic evolution and (b) *MaP+GA*: evolution with initial solutions generated using MaP, in generating approximate signed 8×8 multipliers. Each of the sub-figures shows the progression for a different *const_sf*. Each figure shows the distribution of the results for an increasing number of fitness evaluations across 10 runs with varying random seeding. As evident from the figure, the MaP-augmented GA shows much-improved hypervolume and continues improving till more iterations than the more generic GA-based search. It must be

noted that the plots show the progression of the hypervolume of the PPF and not the hypervolume of the VPF.

Fig. 12 shows the comparison of the final hypervolume obtained by three approaches—GA, MaP, MaP+GA—for different constraint scaling factors. While the bar plots in the figure show the PPF hypervolume based on ML-based estimation of PPA and BEHAV metrics of the Pareto-front configurations, the markers show the VPF, based on metrics derived from the actual characterization of the Pareto-front configurations. The MaP+GA results in better PPF hypervolume than GA-only across all scenarios. For loosely constrained problems, MaP-based VPF hypervolume is better/equivalent to other approaches. Overall, we observed up to 21% improvements with *AxOMaP*-based methods compared to generic GA.

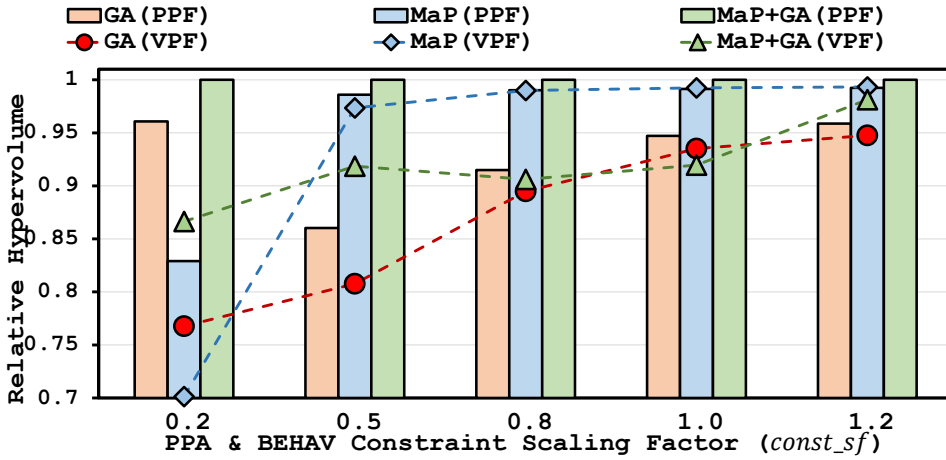


Fig. 12. Comparison of the relative hypervolume of the Pareto-front design points (PPF and VPF) obtained in the minimization of PDPLUT and AVG_ABS_REL_ERR in approximate signed 8×8 multipliers for problems with different levels of maximum PPA and BEHAV constraints.

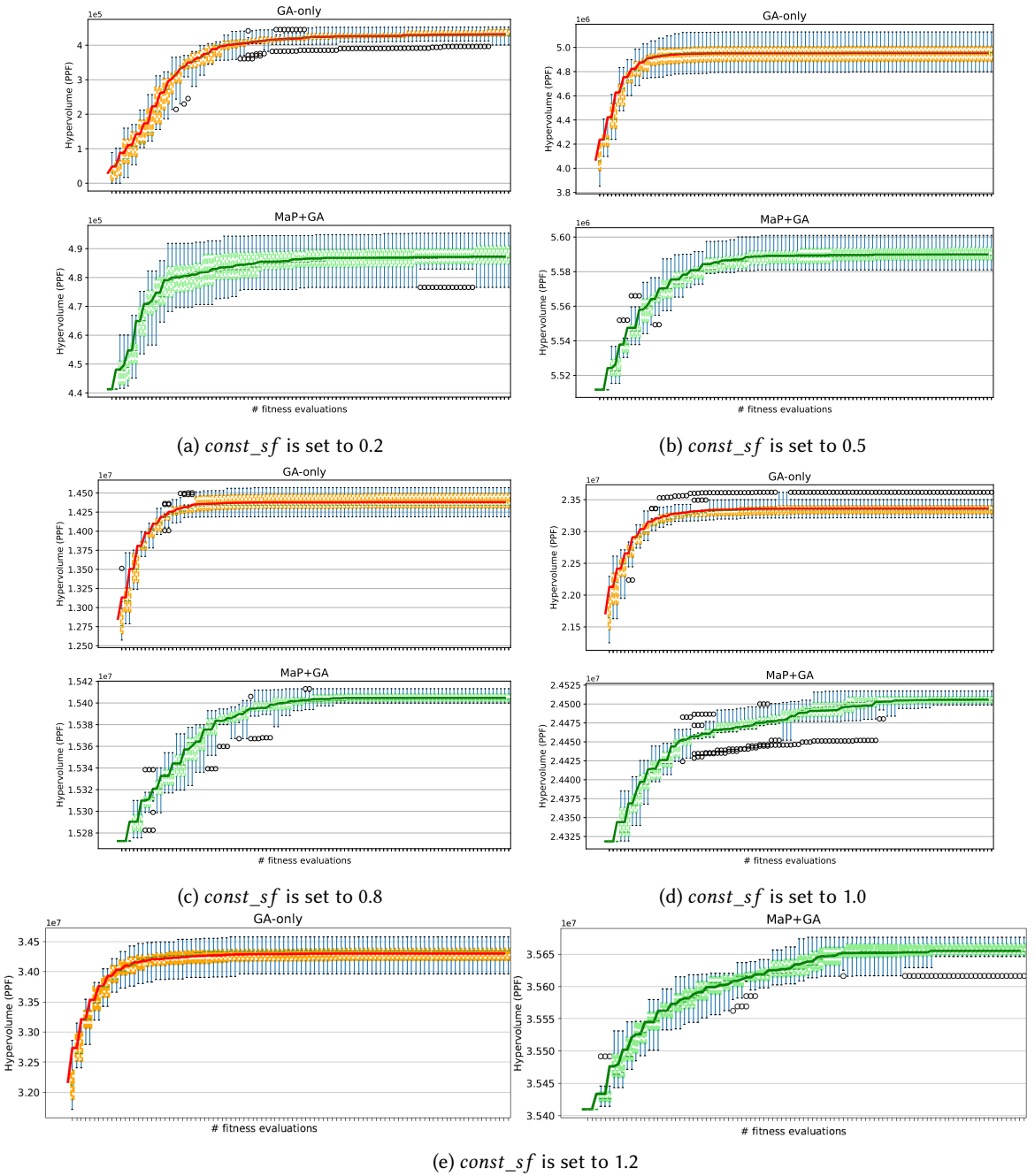


Fig. 13. Progress of the distribution of the hypervolume across 10 different searches reported by generic GA (GA-only) and MaP-augmented GA (MaP+GA) search methods after an equivalent number of increasing fitness evaluations. The line traces the mean.

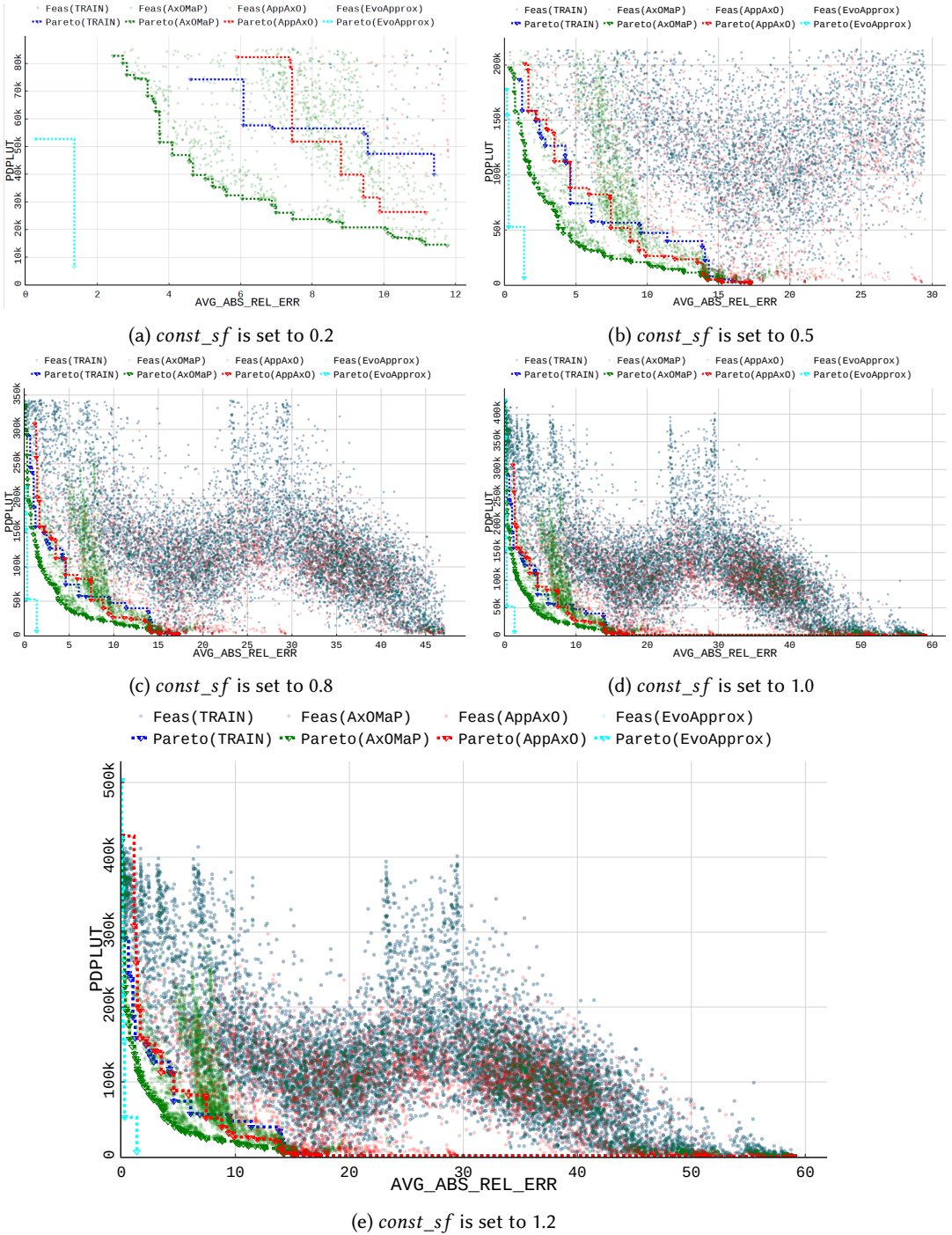


Fig. 14. Comparison of the Pareto-front obtained by *AxOMaP* to that reported in *AppAxO* [25] and *EvoApprox* [10] for approximate signed 8×8 multipliers.

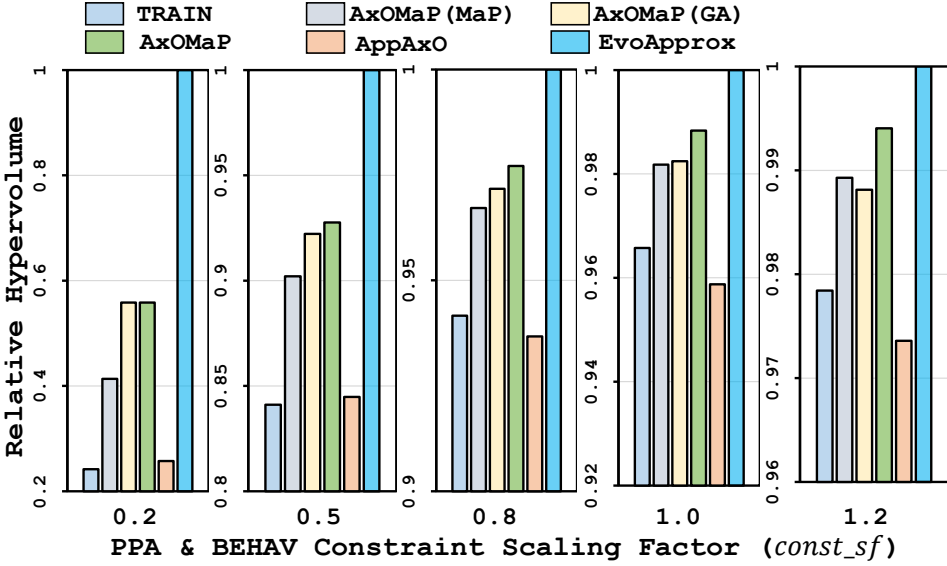


Fig. 15. Comparison of the Pareto-front hypervolume obtained with *AxOMaP* compared to that in related works, for different DSE problems obtained by varying the *const_sf* values

5.4 Comparison with State-of-the-art

5.4.1 Operator-level DSE In order to compare with related state-of-the-art approaches to designing FPGA-based AxOs, we evaluated the proposed methods for both operator-level DSE and application-specific DSE for synthesizing novel approximate signed 8-bit multipliers. Fig. 14 shows the different design points and the Pareto-fronts obtained using the training data in *AxOMaP*, DSE results of *AxOMaP* and the reported results of *EvoApprox* [10] and *AppAxO* [25]. Each sub-figure shows the Pareto-front for a different value of *const_sf*. While in *EvoApprox*, ASIC-optimized logic is synthesized and implemented on FPGAs, the other methods involve optimizing for FPGAs. With *AxOMaP* we report considerably better Pareto-front than *AppAxO*.

The resulting hypervolume of the solutions at different constraint scaling is shown in Fig. 15. All the results correspond to the VPF. As can be seen in the figure, *AxOMaP* methods, both MaP and MaP+GA, result in a better quality of results than those reported in *AppAxO*. We report 116%, 9.8%, 4.3%, 3.1% and 2.1% higher hypervolume than *AppAxO* for *const_sf* values of 0.2, 0.5, 0.8, 1.0, and 1.2 respectively. As evident from both Fig. 14 and Fig. 15, the largest improvement over the designs reported in *AppAxO* occurs in the case of more tightly constrained search. The approximate design configurations obtained from the MaP-based DSE, being solutions of constrained problems themselves, aid in generating better solutions under such tighter constraints. As seen in Fig. 14, with rising tolerance to error (for less tightly constrained problems) more designs are generated with higher cost to accuracy while resulting in lower PDPLUT. It can be noted from Fig. 15, that we report considerable improvements over *AppAxO* [25], the other methodology implementing FPGA-specific LUT-level optimizations.

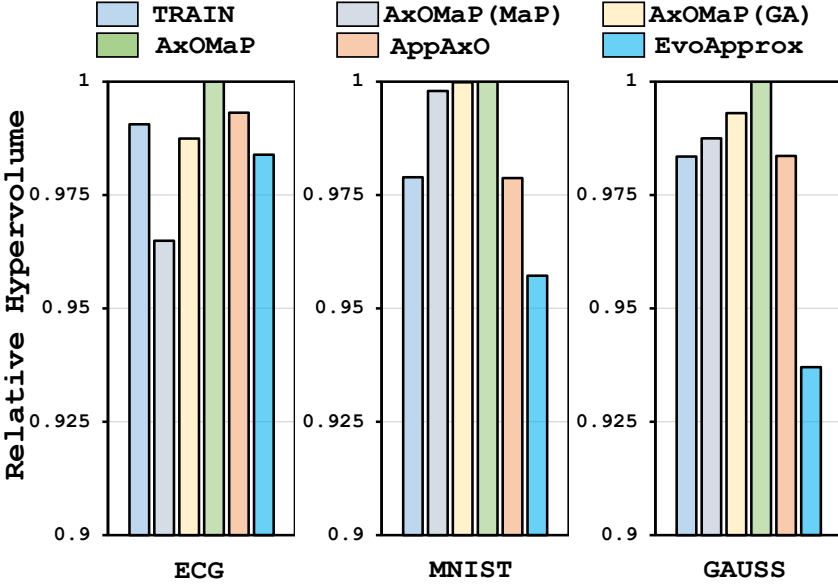


Fig. 16. Pareto-front hypervolume obtained for the application-specific search of approximate signed 8×8 multipliers.

5.4.2 Application-specific DSE As discussed in *AppAxO*, the operator model used does not allow the exploration of the *init values* in the LUTs, as is possible in *EvoApprox* designs. Therefore, the results at the operator-level optimization are worse than that reported with *EvoApprox*. However, the ability to generate more novel designs, by removing a different subset of LUTs, allows the LUT-based optimization methodologies to adapt to any inherent tolerance of different applications. Using the designs generated by *EvoApprox*, on the other hand, limits the exploration to a fixed set of approximate designs.

Consequently, for application-specific DSE we report much better quality of results than both *EvoApprox* and *AppAxO*. Fig. 16 shows the comparison of the resulting hypervolume in the application-specific DSE for three different applications listed in Table 2. While the figure shows the results for an almost unconstrained search (with *const_sf* set to 1.5), with other values of *const_sf* we observe up to 21%, 13%, and 27% better hypervolume than related works for ECG, MNIST, and GAUSS respectively. Fig. 17, Fig. 18 and Fig. 19 show the Pareto front of design points obtained for each of the application for two values of *const_sf*. In the case of ECG, the benefits with *AppAxO* and *AxOMaP* derive from generating designs with large costs to accuracy. For MNIST, *AxOMaP* generates designs with limited improvements over the *AxOMaP*(TRAIN) and *AppAxO*. It can be noted that none of the designs of *EvoApprox* result in feasible designs at tighter constraints (*const_sf* = 0.5). Similarly, for GAUSS only two designs from *EvoApprox* are feasible, with only one design providing any useful benefit (AVG_PSNR_RED < 0).

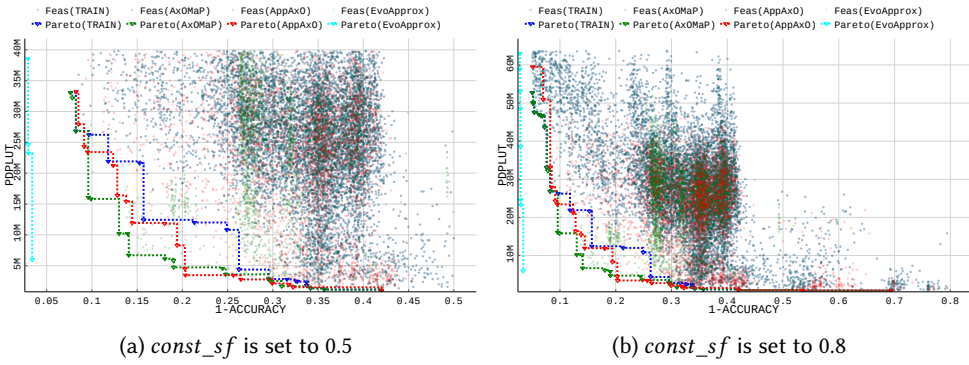


Fig. 17. Pareto-fronts for using approximate signed 8×8 multipliers in the LPF of ECG peak detection.

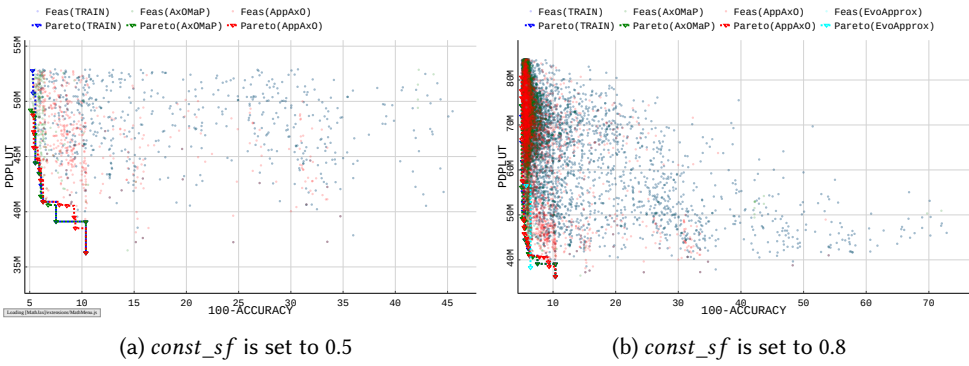


Fig. 18. Pareto-fronts for using approximate signed 8×8 multipliers in the MNIST digit classifier.

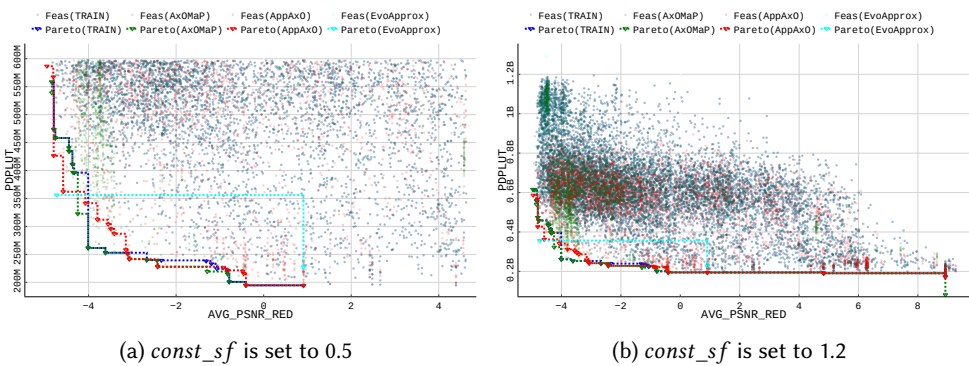


Fig. 19. Pareto-fronts for using approximate signed 8×8 multipliers in 2D gaussian smoothing filter.

6 Conclusion

Approximate computing is one of the more widely researched design approaches for enabling future resource-constrained smart systems. The inherent noise-tolerant behavior of emerging applications such as ML, data mining, etc. provides a conducive environment to approximate computing. However, extracting the maximum benefits with approximate systems for such applications requires DSE approaches that enable a high level of application-specific search, at various levels of the system stack. To this end, the current article, we present a novel methodology for synthesizing FPGA-based approximate operators. The proposed approach leverages the statistical analysis of characterization data to improve the efficacy of prevalent DSE methods. Using the proposed methods, we report up to 116% and 27% improved designs than state-of-the-art approaches for operator-level and application-specific DSE respectively. The proposed methodology can be extended to use more sophisticated analysis methods and operator models for improving the DSE.

References

- [1] Hande Alemdar, Vincent Leroy, Adrien Prost-Boucle, and Frédéric Pétrot. 2017. Ternary neural networks for resource-efficient AI applications. In *2017 International Joint Conference on Neural Networks (IJCNN)*. 2547–2554. <https://doi.org/10.1109/IJCNN.2017.7966166>
- [2] Francesco Biscani and Dario Izzo. 2020. A parallel global multiobjective framework for optimization: PAGMO. *Journal of Open Source Software* 5, 53 (2020), 2338. <https://doi.org/10.21105/joss.02338>
- [3] Zahra Ebrahimi, Salim Ullah, and Akash Kumar. 2020. SIMDive: Approximate SIMD Soft Multiplier-Divider for FPGAs with Tunable Accuracy. In *Proceedings of the 2020 on Great Lakes Symposium on VLSI (Virtual Event, China) (GLSVLSI '20)*. Association for Computing Machinery, New York, NY, USA, 151–156. <https://doi.org/10.1145/3386263.3406907>
- [4] Félix-Antoine Fortin, François-Michel De Rainville, Marc-André Gardner Gardner, Marc Parizeau, and Christian Gagné. 2012. DEAP: Evolutionary Algorithms Made Easy. *J. Mach. Learn. Res.* 13, 1 (jul 2012), 2171–2175.
- [5] Soheil Hashemi, R. Iris Bahar, and Sherief Reda. 2015. DRUM: A Dynamic Range Unbiased Multiplier for approximate applications. In *2015 IEEE/ACM International Conference on Computer-Aided Design (ICCAD)*. 418–425. <https://doi.org/10.1109/ICCAD.2015.7372600>
- [6] Hou-Jen Ko and Shen-Fu Hsiao. 2011. Design and Application of Faithfully Rounded and Truncated Multipliers With Combined Deletion, Reduction, Truncation, and Rounding. *IEEE Transactions on Circuits and Systems II: Express Briefs* 58, 5 (2011), 304–308. <https://doi.org/10.1109/TCSII.2011.2148970>
- [7] Parag Kulkarni, Puneet Gupta, and Milos Ercegovac. 2011. Trading Accuracy for Power with an Underdesigned Multiplier Architecture. In *2011 24th International Conference on VLSI Design*. 346–351. <https://doi.org/10.1109/VLSID.2011.51>
- [8] Sparsh Mittal. 2016. A Survey of Techniques for Approximate Computing. *ACM Comput. Surv.* 48, 4, Article 62 (mar 2016), 33 pages. <https://doi.org/10.1145/2893356>
- [9] Vojtech Mrazek, Muhammad Abdullah Hanif, Zdenek Vasicek, Lukas Sekanina, and Muhammad Shafique. 2019. AutoAx: An Automatic Design Space Exploration and Circuit Building Methodology Utilizing Libraries of Approximate Components. In *Proceedings of the 56th Annual Design Automation Conference 2019 (Las Vegas, NV, USA) (DAC '19)*. Association for Computing Machinery, New York, NY, USA, Article 123, 6 pages. <https://doi.org/10.1145/3316781.3317781>
- [10] Vojtech Mrazek, Radek Hrbacek, Zdenek Vasicek, and Lukas Sekanina. 2017. EvoApprox8b: Library of Approximate Adders and Multipliers for Circuit Design and Benchmarking of Approximation Methods. In *Design, Automation & Test in Europe Conference & Exhibition (DATE), 2017*. 258–261. <https://doi.org/10.23919/DATE.2017.7926993>
- [11] Vojtech Mrazek, Lukas Sekanina, and Zdenek Vasicek. 2020. Libraries of Approximate Circuits: Automated Design and Application in CNN Accelerators. *IEEE Journal on Emerging and Selected Topics in Circuits and Systems* 10, 4 (2020), 406–418. <https://doi.org/10.1109/JETCAS.2020.3032495>
- [12] Eriko Nurvitadhi, Andrew Boutros, Prerna Budhkar, Ali Jafari, Dongup Kwon, David Sheffield, Abirami Prabhakaran, Karthik Gururaj, Pranavi Appana, and Mishali Naik. 2019. Scalable Low-Latency Persistent Neural Machine Translation on CPU Server with Multiple FPGAs. In *2019 International Conference on Field-Programmable Technology (ICFPT)*. 307–310. <https://doi.org/10.1109/ICFPT47387.2019.00054>
- [13] F. Pedregosa, G. Varoquaux, A. Gramfort, V. Michel, B. Thirion, O. Grisel, M. Blondel, P. Prettenhofer, R. Weiss, V. Dubourg, J. Vanderplas, A. Passos, D. Cournapeau, M. Brucher, M. Perrot, and E. Duchesnay. 2011. Scikit-learn: Machine Learning in Python. *Journal of Machine Learning Research* 12 (2011), 2825–2830.

- [14] Nicola Petra, Davide De Caro, Valeria Garofalo, Ettore Napoli, and Antonio G. M. Strollo. 2010. Truncated Binary Multipliers With Variable Correction and Minimum Mean Square Error. *IEEE Transactions on Circuits and Systems I: Regular Papers* 57, 6 (2010), 1312–1325. <https://doi.org/10.1109/TCSL.2009.2033536>
- [15] Aleksandra Płońska and Piotr Płoński. 2021. MLJAR: State-of-the-art Automated Machine Learning Framework for Tabular Data. Version 0.10.3. <https://github.com/mljar/mljar-supervised>
- [16] Bharath Srinivas Prabhakaran, Vojtech Mrazek, Zdenek Vasicek, Lukas Sekanina, and Muhammad Shafique. 2020. ApproxFPGAs: Embracing ASIC-Based Approximate Arithmetic Components for FPGA-Based Systems. In *Proceedings of the 57th ACM/EDAC/IEEE Design Automation Conference (Virtual Event, USA) (DAC '20)*. IEEE Press, Article 118, 6 pages.
- [17] Bharath Srinivas Prabhakaran, Semeen Rehman, Muhammad Abdullah Hanif, Salim Ullah, Ghazal Mazaheri, Akash Kumar, and Muhammad Shafique. 2018. DeMAS: An efficient design methodology for building approximate adders for FPGA-based systems. In *2018 Design, Automation & Test in Europe Conference & Exhibition (DATE)*. 917–920. <https://doi.org/10.23919/DAT.2018.8342140>
- [18] Shvetank Prakash, Tim Callahan, Joseph Bushagour, Colby Banbury, Alan V Green, Pete Warden, Tim Ansell, and Vijay Janapa Reddi. 2022. CFU playground: Full-stack open-source framework for tiny machine learning (tinyml) acceleration on FPGAs. *arXiv preprint arXiv:2201.01863* (2022).
- [19] Rohit Ranjan, Salim Ullah, Siva Satyendra Sahoo, and Akash Kumar. 2023. SyFAXO-GeN: Synthesizing FPGA-Based Approximate Operators with Generative Networks. In *Proceedings of the 28th Asia and South Pacific Design Automation Conference (Tokyo, Japan) (ASPDAC '23)*. Association for Computing Machinery, New York, NY, USA, 402–409. <https://doi.org/10.1145/3566097.3567891>
- [20] Semeen Rehman, Walaa El-Harouni, Muhammad Shafique, Akash Kumar, Jorg Henkel, and Jörg Henkel. 2016. Architectural-Space Exploration of Approximate Multipliers. In *2016 IEEE/ACM International Conference on Computer-Aided Design (ICCAD) (Austin, TX, USA)*. IEEE Press, 1–8. <https://doi.org/10.1145/2966986.2967005>
- [21] Muhammad Shafique, Waqas Ahmad, Rehan Hafiz, and Jörg Henkel. 2015. A low latency generic accuracy configurable adder. In *2015 52nd ACM/EDAC/IEEE Design Automation Conference (DAC)*. 1–6. <https://doi.org/10.1145/2744769.2744778>
- [22] Muhammad Shafique, Rehan Hafiz, Semeen Rehman, Walaa El-Harouni, and Jörg Henkel. 2016. Cross-layer approximate computing: From logic to architectures. In *DAC*.
- [23] Salim Ullah, Sanjeev Sripadraj Murthy, and Akash Kumar. 2018. SMApPoxLib: Library of FPGA-based Approximate Multipliers. In *2018 55th ACM/ESDA/IEEE Design Automation Conference (DAC)*. 1–6. <https://doi.org/10.1109/DAC.2018.8465845>
- [24] Salim Ullah, Semeen Rehman, Muhammad Shafique, and Akash Kumar. 2022. High-Performance Accurate and Approximate Multipliers for FPGA-Based Hardware Accelerators. *IEEE Transactions on Computer-Aided Design of Integrated Circuits and Systems* 41, 2 (2022), 211–224. <https://doi.org/10.1109/TCAD.2021.3056337>
- [25] Salim Ullah, Siva Satyendra Sahoo, Nemath Ahmed, Debabrata Chaudhury, and Akash Kumar. 2022. AppAxO: Designing Application-Specific Approximate Operators for FPGA-Based Embedded Systems. *ACM Trans. Embed. Comput. Syst.* 21, 3, Article 29 (may 2022), 31 pages. <https://doi.org/10.1145/3513262>
- [26] Salim Ullah, Siva Satyendra Sahoo, and Akash Kumar. 2021. CLAppED: A Design Framework for Implementing Cross-Layer Approximation in FPGA-based Embedded Systems. In *2021 58th ACM/IEEE Design Automation Conference (DAC)*. 475–480. <https://doi.org/10.1109/DAC18074.2021.9586260>
- [27] Salim Ullah, Hendrik Schmidl, Siva Satyendra Sahoo, Semeen Rehman, and Akash Kumar. 2021. Area-Optimized Accurate and Approximate Softcore Signed Multiplier Architectures. *IEEE Trans. Comput.* 70, 3 (2021), 384–392. <https://doi.org/10.1109/TC.2020.2988404>
- [28] Swagath Venkataramani, Srimit T. Chakradhar, Kaushik Roy, and Anand Raghunathan. 2015. Approximate Computing and the Quest for Computing Efficiency. In *Proceedings of the 52nd Annual Design Automation Conference (San Francisco, California) (DAC '15)*. Association for Computing Machinery, New York, NY, USA, Article 120, 6 pages. <https://doi.org/10.1145/2744769.2751163>
- [29] Shibo Wang and Pankaj Kanwar. 2019. BFloat16: The secret to high performance on Cloud TPUs. *Google Cloud Blog* (2019).
- [30] Rong Ye, Ting Wang, Feng Yuan, Rakesh Kumar, and Qiang Xu. 2013. On reconfiguration-oriented approximate adder design and its application. In *2013 IEEE/ACM International Conference on Computer-Aided Design (ICCAD)*. 48–54. <https://doi.org/10.1109/ICCAD.2013.6691096>
- [31] Ofir Zafrir, Guy Boudoukh, Peter Izsak, and Moshe Wasserblat. 2019. Q8BERT: Quantized 8Bit BERT. In *2019 Fifth Workshop on Energy Efficient Machine Learning and Cognitive Computing - NeurIPS Edition (EMC2-NIPS)*. 36–39. <https://doi.org/10.1109/EMC2-NIPS53020.2019.00016>